Excimer laser induced quantum well intermixing: a reproducibility study of the process for fabrication of photonic integrated devices

Romain Beal, Vincent Aimez and Jan J. Dubowski*

Interdisciplinary Institute for Technological Innovation (3IT), Department of Electrical and Computer Engineering, Université de Sherbrooke, 3000 boul. de l'Université, Sherbrooke, Québec J1K 0A3, Canada
*jan.j.dubowski@usherbrooke.ca

Abstract: Excimer (ultraviolet) laser-induced quantum well intermixing (UV-Laser-QWI) is an attractive technique for wafer level post-growth processing and fabrication of a variety of monolithically integrated photonic devices. The results of UV-Laser-QWI employed for the fabrication of multibandgap III–V semiconductor wafers have demonstrated the attractive character of this approach although the process accuracy and reproducibility have remained relatively weakly covered in related literature. We report on a systematic investigation of the reproducibility of this process induced with a KrF excimer laser. The influence of both the irradiation with different laser doses and the annealing temperatures on the amplitude of intermixing in InGaAs/InGaAsP/InP quantum well heterostructures has been evaluated based on the photoluminescence measurements. Under optimized conditions, the process allows to blue shift the bandgap of a heterostructure by more than 100 nm with a remarkable 5.3% relative standard deviation.

©2015 Optical Society of America

OCIS codes: (250.0250) Optoelectronics; (140.3390) Laser materials processing; (160.3130) Integrated optics material; (130.3120) Integrated optics devices; (250.5590) Quantum well, -wire and -dot devices; (140.7240) UV, EUV, and X-ray lasers.

References and links

1. H. Soda, M. Furutsu, K. Sato, N. Okazaki, S. Yamazaki, H. Nishimoto, and H. Ishikawa, "High-power and high-speed semi-insulating BH structure monolithic electroabsorption modulator/DFB laser light source," Electron. Lett. **26**(1), 9–10 (1990).
2. F. Kish, R. Nagarajan, D. Welch, P. Evans, J. Rossi, J. Pleumeekers, A. Dentai, M. Kato, S. Corzine, R. Muthiah, M. Ziari, R. Schneider, M. Reffle, T. Butrie, D. Lambert, M. Missey, V. Lal, M. Fisher, S. Murthy, R. Salvatore, S. Demars, A. James, and C. Joyner, "From Visible Light-Emitting Diodes to Large-Scale III-V Photonic Integrated Circuits," Proc. IEEE **101**(10), 2255–2270 (2013).
3. A. Talneau, D. Rondi, M. Krakowski, and R. Blondeau, "Very low threshold operation of 1.52 um GaInAsP/InP DFB buried ridge structure laser diodes entirely grown by MOCVD," Electron. Lett. **24**(10), 609–611 (1988).
4. P. J. Williams, P. M. Charles, I. Griffith, I. Considine, and A. C. Carter, "High performance buried ridge DFB lasers monolithically integrated with butt coupled strip loaded passive waveguides for OEIC," Electron. Lett. **26**(2), 142–143 (1990).
5. C. A. Verschuren, P. J. Harmsma, Y. S. Oei, M. R. Leys, H. Vonk, and J. H. Wolter, "Butt-coupling loss of 0.1dB/interface in InP/InGaAs MQW waveguide-waveguide structures grown by selective area chemical beam epitaxy," J. Cryst. Growth **188**(1-4), 288–294 (1998).
6. M. Gibbon, J. P. Stagg, C. G. Cureton, E. J. Thrush, C. J. Jones, R. E. Mallard, R. E. Pritchards, N. Collis, and A. Chew, "Selective-area low-pressure MOCVD of GaInAsP and related materials on planar InP substrates," Semicond. Sci. Technol. **8**(6), 998–1010 (1993).
7. J. J. Coleman, R. M. Lammert, M. L. Osowski, and A. M. Jones, "Progress in InGaAs - GaAs Selective-Area MOCVD Toward Photonic Integrated Circuits," IEEE J. Sel. Top. Quant. **3**(3), 874–884 (1997).

#226737 - $15.00 USD Received 12 Nov 2014; revised 2 Jan 2015; accepted 9 Jan 2015; published 16 Jan 2015

8. M. J. R. Heck, J. F. Bauters, M. L. Davenport, J. K. Doylend, S. Jain, G. Kurczveil, S. Srinivasan, Y. Tang, and J. E. Bowers, "Hybrid Silicon Photonic Integrated Circuit Technology," IEEE J. Sel. Top. Quant. **19**(4), 6100117 (2013).
9. H.-H. Chang, Y. H. Kuo, R. Jones, A. Barkai, and J. E. Bowers, "Integrated hybrid silicon triplexer," Opt. Express **18**(23), 23891–23899 (2010).
10. S. R. Jain, M. N. Sysak, G. Kurczveil, and J. E. Bowers, "Integrated hybrid silicon DFB laser-EAM array using quantum well intermixing," Opt. Express **19**(14), 13692–13699 (2011).
11. H. Li, *Semiconductor Quantum Wells Intermixing* (Gordon and Breach Science Publishers, 2000).
12. W. D. Laidig, N. Holonyak, M. D. Camaras, K. Hess, J. J. Coleman, P. D. Dapkus, and J. Bardeen, "Disorder of an AlAs-GaAs superlattice by impurity diffusion," Appl. Phys. Lett. **38**(10), 776 (1981).
13. J. H. Marsh, "Quantum well intermixing," Semicond. Sci. Technol. **8**(6), 1136–1155 (1993).
14. R. Stanowski, M. Martin, R. Ares, and J. J. Dubowski, "Iterative bandgap engineering at selected areas of quantum semiconductor wafers," Opt. Express **17**(22), 19842–19847 (2009).
15. C. J. McLean, J. H. Marsh, R. M. De La Rue, A. C. Bryce, B. Garrett, and R. W. Glew, "Layer selective disordering by photoabsorption-induced thermal diffusion in InGaAs/InP based multiquantum well structures," Electron. Lett. **28**(12), 1117–1119 (1992).
16. H. S. Djie and T. Mei, "Plasma-induced quantum well intermixing for monolithic photonic integration," IEEE J. Sel. Top. Quant. **11**(2), 373–382 (2005).
17. V. Aimez, J. Beauvais, J. Beerens, D. Morris, H. S. Lim, and Boon-Siew Ooi, "Low-Energy Ion-Implantation-Induced Quantum-Well Intermixing," IEEE J. Sel. Top. Quant. **8**(4), 870–879 (2002).
18. S. C. Du, L. Fu, H. H. Tan, and C. Jagadish, "Investigation of ion implantation induced intermixing in InP based quaternary quantum wells," J. Phys. D Appl. Phys. **44**(47), 475105 (2011).
19. B. S. Ooi, C. J. Hamilton, K. McIlvaney, A. C. Bryce, R. M. De La Rue, J. H. Marsh, and J. S. Roberts, "Quantum- Well Intermixing in GaAs-AlGaAs Structures Using Pulsed Laser Irradiation," IEEE Photonic. Tech. L. **9**(5), 587–589 (1997).
20. A. McKee, C. J. McLean, G. Lullo, A. C. Bryce, R. M. De La Rue, J. H. Marsh, and C. C. Button, "Monolithic integration in InGaAs-InGaAsP multiple-quantum-well structures using laser intermixing," IEEE J. Quantum Electron. **33**(1), 45–55 (1997).
21. K. Brunner, U. Bockelmann, G. Abstreiter, M. Walther, G. Böhm, G. Tränkle, and G. Weimann, "Photoluminescence from a Single GaAs/AlGaAs Quantum Dot," Phys. Rev. Lett. **69**(22), 3216–3219 (1992).
22. J. Genest, J. J. J. Dubowski, V. Aimez, N. Pauc, D. Drouin, and M. Post, "UV laser controlled quantum well intermixing in InAlGaAs/GaAs heterostructures," J. Phys. Conf. Ser. **59**, 605–609 (2007).
23. J. Genest, R. Beal, V. Aimez, and J. J. Dubowski, "ArF laser-based quantum well intermixing in InGaAs/InGaAsP heterostructures," Appl. Phys. Lett. **93**(7), 071106 (2008).
24. N. Liu, S. Poulin, and J. J. Dubowski, "Enhanced photoluminescence emission from bandgap shifted InGaAs/InGaAsP/InP microstructures processed with UV laser quantum well intermixing," J. Phys. D Appl. Phys. **46**(44), 445103 (2013).
25. N. Liu and J. J. Dubowski, "Chemical evolution of InP/InGaAs/InGaAsP microstructures irradiated in air and deionized water with ArF and KrF lasers," Appl. Surf. Sci. **270**, 16–24 (2013).
26. M. Kaleem, X. Zhang, Y. Zhuang, J.-J. He, N. Liu, and J. J. Dubowski, "UV laser induced selective-area bandgap engineering for fabrication of InGaAsP/InP laser devices," Opt. Laser Technol. **51**, 36–42 (2013).
27. M. Kaleem, X. Zhang, Y.-G. Yang, Y. Zhuang, and J. J. He, "Multi-bandgap photonic materials and devices fabricated by UV-laser induced quantum well intermixing," Optoelectronics Lett. **9**(5), 358–361 (2013).
28. J. E. Haysom, *Quantum Well Intermixing of InGaAs(P)/InP Heterostructures* (2001).
29. N. Itoh and A. M. Stoneham, "Treatment of semiconductor surfaces by laser-induced electronic excitation," J. Phys. Condens. Matter **13**, R489–R503 (2001).
30. S. Charbonneau, E. S. Koteles, P. J. Poole, J. J. He, G. C. Aers, J. Haysom, M. Buchanan, Y. Feng, A. Delage, F. Yang, M. Davies, R. D. Goldberg, P. G. Piva, and I. V. Mitchell, "Photonic integrated circuits fabricated using ion implantation," IEEE J. Sel Top Quant **4**(4), 772–793 (1998).
31. J. Kanasaki, A. Okano, K. Ishikawa, Y. Nakai, and N. Itoh, "Defect-Initiated Emission of Ga Atoms from the Gaas (110) Surface-Induced by Pulsed-Laser Irradiation," J. Phys. Condens. Matter **5**(36), 6497–6506 (1993).

1. Introduction

Over the past 25 years, the complexity of photonic integrated devices has progressed from a simple laser-modulator architecture [1] to wavelength division multiplexing transmitter/receiver devices with several hundreds of components integrated within the same wafer [2]. Such devices require the coexistence of different heterostructures suitable to deliver a plethora of functions handled by a photonic integrated circuit (PIC). The most obvious approach allowing such functions is based on the epitaxial growth of wafers that, through a series of etch-and-re-growth steps, could deliver multi-bandgap wafers [3–5]. However, the regrowth techniques rely on so-called butt-joint architecture, and thus are relatively complex and frequently encounter difficulties in delivering high-quality interfaces.

#226737 - $15.00 USD Received 12 Nov 2014; revised 2 Jan 2015; accepted 9 Jan 2015; published 16 Jan 2015
© 2015 OSA

Selective area growth (SAG) [6, 7] is an alternative method that allows limiting the number of re-growth steps by employing dielectric masks to control the thickness of nearby growing layers. The weak point of this technique concerns the difficulty in controlling the thickness of a layer in the vicinity of a dielectric mask. Hybrid integration is a seemingly promising lead which takes advantage of a relatively low cost of silicon for the passive sections and III/V heterostructures for active operations [8]. Devices emitting over a large spectrum may however require several active bandgap structures. Such devices can be obtained by bonding either different heterostructures on the same silicon wafer [9] or by interfacing with a single structure previously processed by quantum well intermixing (QWI) [10].

The QWI process is a post growth technique designed to modify the bandgap energy profile of an existing quantum well (QW) system by intermixing the species of the barriers and the wells [11]. While rapid thermal annealing (RTA) is applied to activate intermixing-promoting point defects, a selective area intermixing is achieved by introducing point defects in selective areas of the investigated QW wafers. QWI brings less complexity over epitaxial etch-regrowth processes and increases versatility in desired wafer bandgap tuning. Thus, the QWI process could deliver multi-bandgap wafers rapidly and, potentially, at an attractive manufacturing cost. Examples of QWI approaches include impurity induced disordering (IID) [12], impurity free vacancy disordering (IFVD) [13], infrared laser annealing [14] [also known as photon absorption induced disordering (PAID)] [15], plasma induced intermixing [16] and ion implantation induced intermixing [17, 18]. Among these processes, ultraviolet laser-induced quantum well intermixing (UV-Laser-QWI) is particularly appealing due to its ability to produce selective area bandgap tuned wafers without employing contact masking and associated processing steps. In addition to pulsed IR laser QWI [19, 20], both visible [21] and pulsed UV [22, 23] lasers have been investigated for the intermixing and selective are bandgap engineering.

The influence of different environments on UV-Laser-QWI, such as air, SiO_2 and deionized water has been investigated, demonstrating significant blue shifts with a minimal modification of the quality of InP/InGaAs/InGaAsP QW microstructures [23–25]. These experiments have revealed that laser irradiation in air leads to the formation of the InP_xO_y compound on the surface of a cap InP material, while irradiation in water leads to only a partially decomposed InP cap whose stoichiometry is restored following the rapid thermal annealing (RTA) step. Consistent with this observation are relatively large bandgap blue shifts (:130 nm) found in microstructures processed in air with the excimer UV-Laser-QWI technique [25, 26]. An example of the successful application of such an approach for device fabrication are high-intensity InGaAsP/InP laser diodes [27]. To address the potential of the QWI method for industrial applications, it is mandatory to investigate its reproducibility based on a relatively large sampling. Related to this has been a reproducibility study of the ion implantation induced QWI [28]. Here, we discuss the results related to UV-Laser-QWI reproducibility in samples irradiated with a KrF laser in an air environment. Due to the possibility of the laser irradiating numerous sites on the same sample, the number of investigated sites for that purpose was equivalent to 217 samples that would have to be processed with an alternative (laser-free) QWI technique.

2. Experimental details

The experiments were carried out using 5-QW InGaAs/InGaAsP laser heterostructures grown by MOCVD on 3-inch diameter InP substrates. The heterostructures, designed for the fabrication of laser devices emitting at a 1.55 μm wavelength, were capped with a 200 nm undoped InP sacrificial layer. After completion of the intermixing process, this layer was removed by wet etching, which allowed achieving samples with a minimized concentration of surface defects. A cross-section of the investigated heterostructures is shown in Fig. 1.

Prior to laser irradiation, the samples were submitted to solvent cleaning (successively in Opticlear, acetone and isopropanol) using an ultrasonic bath. The samples were irradiated in

#226737 - $15.00 USD Received 12 Nov 2014; revised 2 Jan 2015; accepted 9 Jan 2015; published 16 Jan 2015
© 2015 OSA

an air environment with a KrF (248 nm) excimer laser (GSI Lumonics PM-848). The laser produced 20 ns pulses of fluence extending up to 380 mJ/pulse. A typical energy root mean square (RMS) variation of the fluence, measured for 290 mJ/pulse, was estimated at 2.6% over an hour of operation at a 2 Hz repetition rate. A beam delivery system comprising a fly-eye-array homogenizer allowed producing top hat shape pulses with σRMS intensity of 5% over an area of 15 mm x 11 mm. Rectangular 3 mm x 2.25 mm and round 3 mm diameter masks were placed in the plane of the laser homogenized beam and projected on the sample surface with a demagnification ratio of 1.6. Samples were irradiated with a fixed pulse fluence of 155 mJ/cm^2 and the intermixing amplitude was controlled by changing the total number of irradiating pulses. While lower laser fluence irradiation has been reported to promote intermixing [25], this particular value was chosen based on experimental evidence indicating that a slightly increased fluence improves intermixing homogeneity within the processed site.

Layer
200 nm InP **sacrificial layer** U/D
100 nm InGaAs **contact layer** p$^+$ Zn 8 x 10^{18} cm^{-3}
50 nm InGaAsP 1.2Q p$^+$ Zn 2 x 10^{18} cm^{-3}
1200 nm InP **upper cladding** p Zn 6 x 10^{17} cm^{-3}
10 nm 1.3Q InGaAsP **etch stop** p Zn 6 x 10^{17} cm^{-3}
100 nm InP p Zn 6 x 10^{17} cm^{-3}
80 nm InGaAsP 1.05Q **upper waveguiding core** n Si 5 x 10^{17} cm^{-3}
50 nm InGaAsP 1.2Q n Si 5 x 10^{17} cm^{-3}
12 nm InGaAsP **barrier** 1.25Q U/D
5 nm InGaAs **quantum well** U/D (X 5)
12 nm InGaAsP **barrier** 1.25Q U/D (X 5)
50 nm InGaAsP 1.2Q n Si 5 x 10^{17} cm^{-3}
80 nm InGaAsP 1.05Q **lower waveguiding core** n Si 5 x 10^{17} cm^{-3}
1400 nm InP **lower cladding** n$^+$ Si 2 x 10^{18} cm^{-3}
InP **substrate** n$^+$ S 2 x 10^{18} cm^{-3}

Fig. 1. Cross-section of the 5-QW laser heterostructure employed for a reproducibility study of the UV-Laser-QWI process.

The number of pulses delivered by the laser on the sample surface ranged from 1 to 150. After laser irradiation, the samples, each comprising between 6 and 25 sites, were annealed individually at 670 C for 2 minutes. The RTA step was carried out using a 30 kW JIPELEC Jetfirst thermal processor with the process temperature induced with infrared lamps and monitored by a chromel/alumel thermocouple. A 4-inch 350-µm thick silicon wafer was used to support the annealed samples. Quartz rods fixed in the RTA chamber were used to support the wafer itself. The samples were placed face down on the silicon substrate to minimize material desorption. Also, to minimize the effect of potential temperature variations along the wafer, the samples were installed, each time, at nominally same location with respect to the location of the temperature monitoring thermocouple. The RTA process was performed in forming gas environment (N_2:H_2, 9:1). The samples' photoluminescence (PL) was measured before and after intermixing using a Philips PLM-150 industrial PL mapping system. The measurements were performed at room temperature using a 1064 nm Nd:YAG laser as an excitation source. By measuring the variation of PL peak position (blue shift), these measurements allowed us to investigate indirectly the modification of the QW concentration profile for each laser processed site.

3. Results and discussion

A total of 12 samples were processed, exhibiting 217 PL blue shift values for different laser doses. Figure 2 shows blue shifts ($|\Delta\lambda|$) measured as a function of pulse number for all the

#226737 - $15.00 USD Received 12 Nov 2014; revised 2 Jan 2015; accepted 9 Jan 2015; published 16 Jan 2015
© 2015 OSA

investigated sites (a), and the average blue shift values as a function of pulse number obtained for a minimum of 4 sites irradiated under the nominally same conditions (b). The PL blue shift evolution displays a rapid increase of the amplitude for laser doses for up to $N = 5$ pulses, which is followed by a weak dependence for $4 \le N < 15$. Within the next 20 pulses, the blue shift amplitude increases about 50%, and it shows relatively stable values for $50 \le N < 70$, followed by a slow decrease for $N > 70$. This decrease is likely concomitant with the onset of laser ablation, which may remove the oxygen rich layer created near the surface of the irradiated material. The removal of such a layer would decrease drastically the amount of point defect participating in the intermixing process during the subsequent RTA step. In addition to the blue shift plateau observed for $4 \le N < 15$, Fig. 2(b) shows another plateau discernible for $50 \le N < 70$ pulses. In the remaining part of this document, we will refer to these as plateau 1 and plateau 2, respectively. The formation of a PL blue shift plateau may be linked to the saturation of the concentration of laser-induced point defects due to the complete removal of ad-atoms [29] and formation of defect clusters that act as traps for point defects, preventing them from diffusing toward the active region and participating in the intermixing process [30]. We note that a 2-plateau evolution was also observed during the ArF-based UV-Laser-QWI process investigated for a similar 5-QW laser heterostructures [23]. It appears that at these conditions, defects that enhance the QWI process have been exhausted and formation of a new type of surface defects begins to take place. For instance, it has been reported that the removal of Ga atoms from the GaAs surface is defect initiated and the irradiation with 1.35 eV laser pulses at 400 mJ/cm^2 could increase and saturate rapidly their removal rate with the pulse number, while for low-fluence pulse irradiation of 200 mJ/cm^2 such a removal rate decreased and saturated at a significantly lower level [31].

A weak dependence of the PL blue shift on the pulse number defines conditions where the UV-Laser-QWI technique could offer the most reproducible results independently from the reproducibility related to the material non-uniformity or the annealing conditions discussed later in this report. Clearly, it is reasonable to expect that the error of $|\Delta\lambda|$ would be minimized when different samples of the investigated QW microstructure were irradiated with $N \approx 10$ and $N \approx 60$ pulses. We have investigated a statistics of the $|\Delta\lambda|$ values observed in the two saturation regions, as these provide an interesting perspective to the application of UV-Laser-QWI for the delivery of multi bandgap wafers with a prominent reproducibility. The $|\Delta\lambda|$ values for each plateau were compiled, giving a total of 67 results for plateau 1 and 37 results for plateau 2. The thermal shift generated in the non-irradiated material was also considered for comparison, based on 12 data points. The related results are presented in Fig. 3. It can be seen that the $|\Delta\lambda|$ values for plateau 1 range between 60 nm and 77 nm, with a mean value of 70.6 nm (± 15%), and a standard deviation of 4.5 nm (6.4%). For plateau 2, the $|\Delta\lambda|$ values range between 91 nm and 113 nm, giving a mean value of 101.5 nm (± 11.3%) and a standard deviation of 5.4 nm (5.3%). At the same time, it can be seen that $|\Delta\lambda|$ for the non-irradiated material ranged between 5 and 8 nm, giving a mean value of 6.7 nm.

We have also investigated the influence of RTA conditions on achieving reproducible QWI results. Figure 4 shows $|\Delta\lambda|$ values observed for a series of samples irradiated with 20 pulses (plateau 1 region) and with 60 pulses (plateau 2 region) that were RTA for 120 s in the temperature range between 640 and 710°C. This figure illustrates also the thermal stability of the non-irradiated material in the same temperature range. It can be seen that $|\Delta\lambda|$ of the non-irradiated material increases from 3 nm at 640°C to 14 nm at 710°C. At the same time, the $|\Delta\lambda|$ amplitude increases linearly between 640 and 690 C, at a rate of 1.8 nm/°C, for both groups of the samples. Taking into account that the RTA process allows to control a set point temperature with ± 5 °C, we estimate that the intended $|\Delta\lambda|$ value can be affected by a related error of up to ± 9 nm.

#226737 - $15.00 USD Received 12 Nov 2014; revised 2 Jan 2015; accepted 9 Jan 2015; published 16 Jan 2015
© 2015 OSA

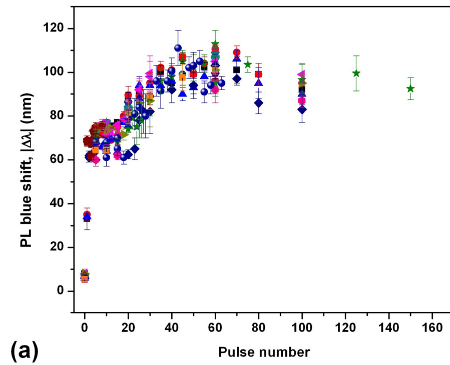

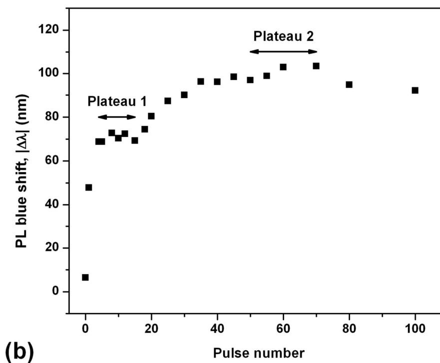

Fig. 2. (a) PL blue shift as a function of pulse number for samples irradiated at 155 mJ/cm^2. The results shown with the same style symbols identify the sites processed on the same sample. (b) Average values of PL blue shift (δblue) collected as a function of pulse number (only data for minimum 4 sites irradiated under the nominally same conditions are taken into account).

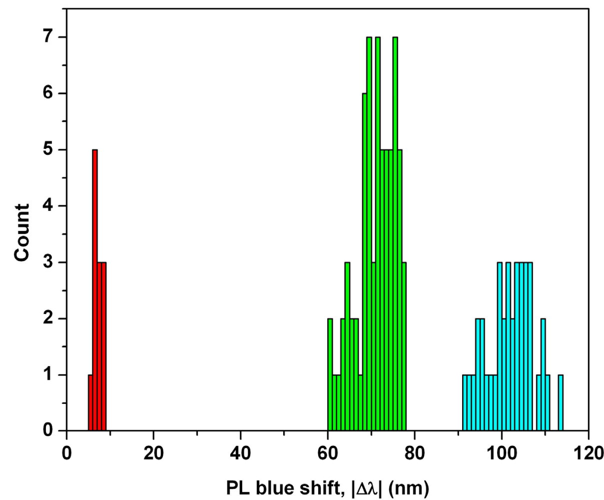

Fig. 3. Distribution of the $|\Delta\lambda|$ values for the unirradiated material (red columns) and samples irradiated with 4-15 pulses (green columns) and 50-70 pulses (blue columns).

#226737 - $15.00 USD Received 12 Nov 2014; revised 2 Jan 2015; accepted 9 Jan 2015; published 16 Jan 2015
© 2015 OSA

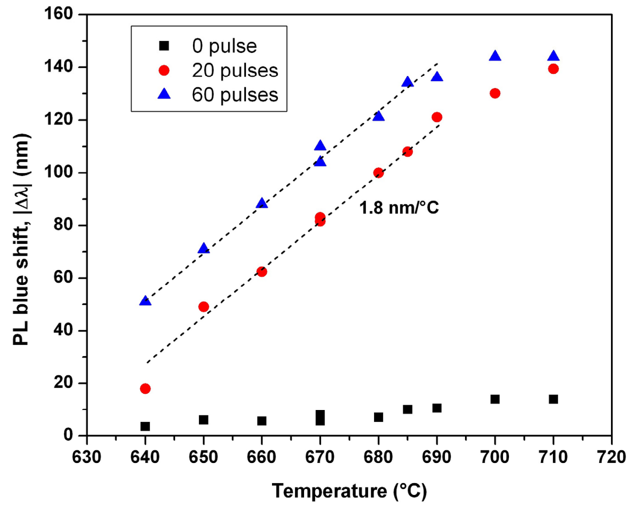

Fig. 4. PL determined blue shift as a function of the RTA temperature for as-received material (■) and sites annealed with 20 (●) and 60 (▲) pulses.

With the analysis of the impact of annealing temperature on the blue shift amplitude, more insight can be provided regarding the UV-Laser-QWI process reproducibility under improved annealing conditions. Hence, two samples were processed with a series of laser irradiated sites. Similarly to previous experiments, the samples were irradiated in air environment with a pulse fluence of 157 mJ/cm^2 projected on 1.1 mm square sites. The first sample was processed at 34 different sites, each with 15 pulses (corresponding to plateau 1) and the second was processed at 30 different sites, each with 60 pulses (corresponding to plateau 2). Both samples were then annealed at 670°C for 2 min. By processing 2 samples, each with a series of sites irradiated with the same number of pulses, a more accurate evaluation of uncertainty of the $|\Delta\lambda|$ amplitude related to the laser process alone, free of RTA variations, could be carried out. The related results are presented in Fig. 5.

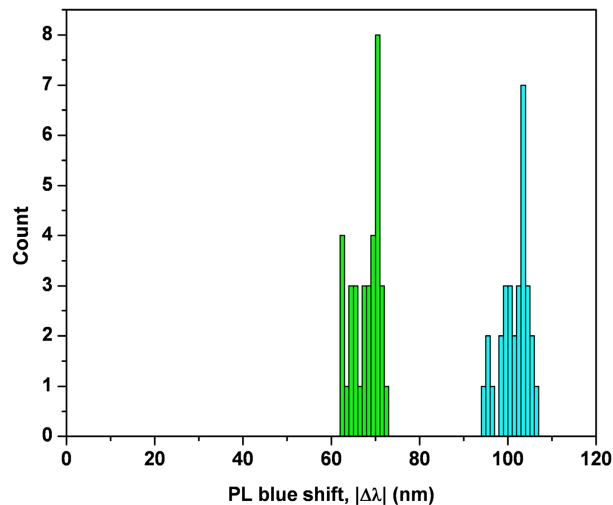

Fig. 5. Distribution of the $|\Delta\lambda|$ values for two samples irradiated at 34 sites with 15 pulses (green columns) and 30 sites with 50-70 pulses (blue columns) respectively.

#226737 - $15.00 USD Received 12 Nov 2014; revised 2 Jan 2015; accepted 9 Jan 2015; published 16 Jan 2015
© 2015 OSA

For the sites of the plateau 1 sample, $|\Delta\lambda|$ amplitude ranged from 62 to 72 nm for a 67.4 nm mean value and for the sites of the plateau 2 sample, it ranged from 94 nm to 106 nm for a 101 nm mean value. These values are consistent with the data discussed in Fig. 2. For the plateau 1 and 2 samples, the standard deviation was determined as 3.1 nm (4.6%) and 3.2 nm (3.2%), respectively. Thus, the reproducibility of $|\Delta\lambda|$ from site to site on such samples was found to be superior to that observed for the set of 12 separate samples processed nominally under the same conditions, but annealed separately. The corresponding maximum variation range decreased from ± 15% to ± 7.9% for the plateau 1, and from ± 11.3% to ± 6.9% for the plateau 2, while the relative standard deviation decreased from 6.4% to 4.6% for the plateau 1 and from 5.3% to 3.2% for the plateau 2.

4. Conclusion

We have investigated reproducibility and the precision of the QWI process induced with the UV-Laser-QWI technique. The samples of a wafer with InGaAs/InGaAsP/InP 5-QW laser heterostructures were laser processed in air environment and annealed in a commercial RTA instrument. The PL blue shift evolution as a function of delivered pulse number exhibited two plateaus, defined between 4 and 15 pulses, and between 50 and 70 pulses.

The results have demonstrated that material with quantum well bandgap blue shifted by 70.6 nm (first plateau) and 101.5 nm (second plateau) can be delivered within ± 15% and ± 11.3%, respectively.

The RTA temperature control was revealed to be of critical importance for achieving high control of the blue shift amplitude. In the temperature range of 640-690 °C, the heterostructure PL determined bandgap varied at the rate of 1.8 nm/°C, which for the RTA system capable of controlling a set point temperature with ± 5 °C, resulted in the bandgap uncertainty of ± 9 nm. When delivering a 2-bandgap material using the UV-Laser-QWI process applied to the same wafer, the bandgap could be delivered within ± 7.9% (± 15% on independently RTA samples) for the plateau 1 region, and within ± 6.9% (± 11.3% on independently RTA samples) for the plateau 2 region. Thus, we have demonstrated that the application of the UV-Laser-QWI process for bandgap engineering of InGaAs/InGaAsP/InP QW laser heterostructures has the potential to deliver 3-bandgap material, consisting of a background and 2 plateau regions sections, with blue shifted amplitudes controlled to better than ± 8%. Such feature is considered highly attractive for the fabrication of advanced multi-bandgap materials at the wafer level in the absence of successive microfabrication steps.

Acknowledgments

This research was supported by the Canada Research Chair in Quantum Semiconductors Program, NanoQuébec and Le Fonds Québécois de la recherche sur la nature et les technologies. Semiconductor wafers, whose acquisition was partially supported by CMC Microsystems (Kingston, Ontario), were grown at the Canadian Photonics Fabrication Centre (Ottawa, Canada). The authors would like to thank the staff of the Université de Sherbrooke Interdisciplinary Institute for Technological Innovation (3IT) for providing technical support as well as Dr. Khalid Moumanis for helping to operate the excimer laser system.